Lab on a Chip

Parallel Multiphase Nanofluidics Utilizing Nanochannel with Partial Hydrophobic Surface Modification and Application to Femtoliter Solvent Extraction

Journal:	*Lab on a Chip*
Manuscript ID	LC-ART-08-2019-000793.R1
Article Type:	Paper
Date Submitted by the Author:	09-Sep-2019
Complete List of Authors:	Kazoe, Yutaka; The University of Tokyo, Ugajin, Takuya; The University of Tokyo Ohta, Ryoichi; The University of Tokyo, Mawatari, Kazuma; The University of Tokyo, Kitamori, Takehiko; The University of Tokyo,

Parallel Multiphase Nanofluidics Utilizing Nanochannel with Partial Hydrophobic Surface Modification and Application to Femtoliter Solvent Extraction

Yutaka Kazoe,[1] Takuya Ugajin,[1] Ryoichi Ohta,[2] Kazuma Mawatari[1] and Takehiko Kitamori[1,*]

[1]Department of Applied Chemistry, School of Engineering, The University of Tokyo, 7-3-1 Hongo, Bunkyo, Tokyo 113-8656, Japan.

[2]Department of Bioengineering, School of Engineering, The University of Tokyo, 7-3-1 Hongo, Bunkyo, Tokyo 113-8656, Japan.

*E-mail: kitamori@icl.t.u-tokyo.ac.jp; Fax: +81 3 5841 6039

Abstract

In the field of microfluidics, utilizing parallel multiphase flows with immiscible liquid/liquid or gas/liquid interfaces along a microchannel has achieved the integration of various chemical processing for analyses and syntheses. Recently, our group has developed nanofluidics that exploits 100 nm nanochannels to realize ultra-small (aL- to fL scale) and highly-efficient chemical operations. Novel applications such as analyses of single cell or even molecules are anticipated. However, the formation of parallel multiphase flows in a nanochannel remains challenging. To this end, here we developed a novel method for nanoscale partial hydrophobic surface modification of a nanochannel utilizing a focused ion beam. Hydrophobic

and hydrophilic areas could be patterned beside one another even in a 60 nm glass nanochannel. Because these patterning maintained the liquid/liquid interface in the nanochannel based on the difference of wettability, stable aqueous/organic parallel two-phase flow in a 40 fL nanochannel was realized for the first time. Utilizing this flow, nanoscale unit operations involving phase confluence, extraction and phase separation were integrated to demonstrate solvent extraction of a lipid according to the Bligh-Dyer method, which is a broadly used pretreatment processing in lipidomics. We accomplished the separation of a lipid and an amino acid in a sample volume of 4 fL (250 times smaller than the pL volume of a single cell) with a processing time of 1 ms (10,000 times faster than that in a microchannel). This study therefore provides a technological breakthrough that advances the field of nanofluidics to allow multiphase chemical processing at fL volumes.

1. Introduction

Multiphase microfluidics have been widely used to perform miniaturized chemical analyses and syntheses.[1] Utilizing parallel multiphase flows with immiscible liquid/liquid or gas/liquid interfaces along a channel is an approach to multiphase microfluidics,[2,3] as well as utilizing droplet or plug flows typically for volume control and compartmentalization to perform highly-efficient reactions[4,5] and chemical processing based on droplet fusion.[6,7] Parallel multiphase flows occur in small spaces in which the effects of viscous force and surface tension are significant, and involve a balance between the fluid pressure and the Laplace pressure derived from surface tension. Because the gas/liquid or liquid/liquid interface

remains at a predetermined position, and because such systems are readily connected to a subsequent operation after phase separation, the use of parallel multiphase flows is advantageous when designing chemical processing in a continuous flow system. Our group has previously proposed an integration method, which we term micro unit operations (MUOs).[8] By connecting MUOs such as microscale mixing, extraction and reaction, in parallel or in series utilizing parallel multiphase flows, various chemical processing including solvent extraction,[9-11] purification,[12,13] synthesis of polymer membranes[14] and environmental analysis,[8] has been miniaturized and integrated.

Recently, our group has applied methods of microfluidics to spaces with dimensions of 10-1000 nm, and has pioneered nanofluidics that exploits nanochannels with well-defined dimensions.[15,16] Nanospaces, in which surface effects are dominant, can be employed to realize novel ultra-small (aL-fL scale) and highly-efficient chemical applications such as single molecule immunoassay,[17] single DNA molecule sorting,[18] femtoliter chromatography,[19] and micro-fuel cells with high proton conductivity.[20] The use of multiphase flows in nanochannels is expected to expand the range of applications by nanofluidics. As an example, in previous work, aL-fL volume aqueous-liquid droplets were formed within an organic phase filled in nanochannels,[21,22] and used to perform single molecule enzyme analyses.[23]

Despite the work of nanofluidics noted above, the formation of parallel multiphase flows in nanochannels has not yet been achieved. Because the Laplace pressure in 100 nm spaces is in the range of 100-1000 kPa, (which is 100-1000 times higher than the pressures in microspaces due to the inversely proportional relationship between pressure and size), it is difficult to balance the fluid and Laplace

pressures to maintain the liquid/liquid or gas/liquid interfaces along the nanochannel. For this issue, our group has developed a potential approach using hydrophobic surface patterning, on which the Laplace pressure works to recover the liquid/liquid or gas/liquid interface.[24] We have realized even countercurrent aqueous/organic parallel two-phase flow in a microchannel.[25] Although this approach is expected to work in nanofluidics because the high Laplace pressure can be effectively used, surface patterning of the 100-1000 nm nanochannels is exceedingly difficult simply because of the small dimensions involved. Typical optical methods[26,27] cannot achieve nanoscale surface patterning due to the optical diffraction limit and challenges related to the alignment of the optical mask. Recently, femtosecond laser-based fabrication methods utilizing nonlinear multiphoton absorption have been developed to achieve fabrication of micro- and nanostructures even in closed spaces like microchannels,[28,29] but the resolution is still insufficient for precise patterning inside nanochannels. Although dip-pen nanolithography[30] allows nanoscale patterning, this method is not readily applicable to a three-dimensional structure such as a nanochannel.

As a means of realizing parallel multiphase flows in nanochannels to provide a new approach to nanofluidics, the present study developed a method of nanoscale partial hydrophobic surface modification in a nanochannel utilizing a focused ion beam (FIB). Using a partially hydrophobic nanochannel produced by the proposed method, the formation of aqueous/organic parallel two-phase flow at fL volumes was verified for the first time. In addition, the parallel two-phase flow in the nanochannel was applied to the solvent extraction of lipid molecules via the Bligh-Dyer method,[31] which is known as an important pretreatment processing in lipidomics. The results obtained in this study will contribute to the

advancement of nanofluidics based on multiphase flow systems in terms of integrating chemical processing at fL volumes with high efficiency.

2. Principle and Fabrication Method

Figure 1(a) provides a schematic showing the formation of aqueous/organic parallel two-phase flow in a nanochannel following partial hydrophobic surface modification. Based on the assumption that the channel depth, d, is much smaller than the channel length, the Laplace pressure, P_{LP}, at the liquid/liquid interface is given by the Young-Laplace equation, $P_{LP} = 2\gamma\cos\theta/d$, where γ is the surface tension and θ is the contact angle. For a channel depth of 100 nm, the Laplace pressure will be in the range of 100-1000 kPa. In this partially hydrophobic nanochannel, the high Laplace pressure can be effectively utilized to produce a parallel two-phase flow by flowing aqueous and organic phases through hydrophilic and hydrophobic areas, respectively, that have been patterned beside one another along the channel. As illustrated in Fig. 1(a), when the pressure of the aqueous phase, P_{aq}, is higher than that of the organic phase, P_{org}, the fluid pressure, P_f, is directed towards the organic phase (such that $P_f = P_{aq} - P_{org} > 0$). In this case, the Laplace pressure is directed towards the aqueous phase and acts to recover the interface ($P_{LP} < 0$). In contrast, when P_{aq} is lower than P_{org} ($P_f < 0$), the Laplace pressure is directed towards the organic phase ($P_{LP} > 0$). In this manner, the Laplace pressure always works to stabilize the parallel two-phase flow.

As a means of rendering the nanochannel surface partially hydrophobic, a nanoscale hydrophobic

surface patterning method was proposed. FIB was employed to overcome the optical diffraction limit, and the nanochannel itself was used as a mask to solve the problem of alignment. Figure 1(b) illustrates the fabrication of hydrophilic and hydrophobic areas patterned side by side along the nanochannel. In this process, a nanochannel is fabricated on a glass substrate with a sputtered chromium layer, after which the surface is modified by hydrophobic molecules. Subsequently, the substrate is inclined to produce a shadowed area as a mask for the FIB process and a focused Ga^+ ion beam is employed to remove the hydrophobic modification on the channel wall. By this process, the FIB-irradiated area returns to the hydrophilic glass surface, and a hydrophobic/hydrophilic surface patterning is achieved. After liftoff by removing the chromium layer, the substrate is bonded to another substrate. Details of this fabrication process are described in the following section. This method allows a nanoscale hydrophobic/hydrophilic surface patterning of a nanochannel with high reproducibility, together with precise control of the modified area by changing the angle of inclination.

3. Experimental

3.1. Fabrication of the nanofluidic device

Based on top-down fabrication methods previously established by our group[32,33] and the proposed modification method (Fig. 1(b)), we developed a process for the fabrication of a nanofluidic device including a nanochannel with partial hydrophobic modification, as described below.

Utilizing electron beam lithography and dry etching, a nanochannel was fabricated on a fused-silica

glass substrate with a thickness of 0.7 mm (VIO-SILSX, Shin-Etsu Quartz Co., Ltd., Tokyo, Japan) on which a chromium layer was sputtered preliminary. In the electron beam lithography with an instrument (ELS-7500, Elionix, Tokyo, Japan), ZEP-520A (Zeon Corp., Tokyo, Japan) was used as the electron beam resist. After developing the resist, the chromium layer in the area irradiated by the electron beam was removed with an etchant (HICRETCH S-1, Wako Pure Chemical Corp., Osaka, Japan). Finally, dry etching using an instrument (NE-550, ULVAC Co., Ltd., Kanagawa, Japan) was performed, using a mixture of gaseous CHF_3 and SF_6.

Octadecyltrimethoxysilane (ODS) was selected for the partial hydrophobic surface modification in the fabricated nanochannel. Working under an argon atmosphere, ODS was modified on the substrate surface at 140°C for 2 h, following which the substrate was washed by ultrasonication in dry toluene. After the modification, the ODS was partially ablated by FIB (FB2200, Hitachi High-Technologies Corp., Tokyo, Japan) with the beam at an angle of 45°relative to the substrate. During this process, the minimum FIB beam power was employed so that only the ODS on the glass surface was removed, without etching the glass. In the liftoff step, the chromium layer on the substrate was removed by the etchant. The chromium etching time was limited to 3-4 min so as not to damage the ODS modification layer.

To permit the injection of samples into the nanochannel, microchannels were fabricated by photolithography and dry etching on a second fused-silica glass substrate with a thickness of 0.25 mm. This substrate was sufficiently thin to allow for microscopic observation of fluid flows in the nanofluidic device at 100× magnification, as described below. During the photolithography, THB-11N (JSR Corp.,

Tokyo, Japan) was used as a photoresist. After developing the resist, the channel was fabricated by dry etching and 0.6 mm inlet holes were created on the substrate using a diamond-coated drill.

Finally, the glass substrates were bonded together to complete the nanofluidic device. Because the conventional method for bonding fused-silica substrates based on thermal fusion at 1080°C could not be used without damaging the ODS modification layer in the nanochannel, a low temperature bonding method previously developed by our group[33] was employed. Prior to bonding, the 0.25-mm-thick glass substrate containing microchannels was washed with a three-to-one mixture of sulfuric acid and hydrogen peroxide, after which the substrate surface was activated using an oxygen and fluorine plasma. Because these intense washing and plasma activation processes would have removed the ODS layer in the nanochannel, the 0.7-mm-thick glass substrate containing the nanochannel with partial hydrophobic surface modification was instead washed with fuming nitric acid for 8 min. After aligning the microchannels and the nanochannel, the two substrates were bonded at a temperature of 120°C while applying a force of 5000N pressure for 1 h, and heated for10 h.

In order to discuss experimental results, the contact angle on the glass, the plasma-irradiated glass, and the ODS-modified surfaces was measured by a contact angle meter (DM-500, Kyowa Interface Science Co., Ltd., Saitama, Japan), as listed in Table 1.

3.2. Formation of parallel two-phase flow in the nanochannel

Using the fabricated device, the formation of aqueous/organic parallel two-phase flow in the nanochannel was investigated. Figure 2 illustrates the experimental setup and the design of the

nanochannel. The width, depth and length dimensions of the two-phase flow nanochannel, which was partially modified with ODS, were 1500 nm, 890 nm and 30 μm, respectively. It should be noted that another glass nanochannel of similar size but without the ODS modification was also designed and fabricated, to examine the effect of the partial hydrophobic surface modification on two-phase flow. Inlet nanochannels with width, depth and length dimensions of 750 nm, 890 nm and 300 μm (sufficiently longer than the two-phase flow nanochannel) were connected in front of the phase confluence zone. The longer length of the inlet nanochannels raised the fluidic resistance to prevent the sample from flowing upstream. Following phase separation, the nanochannels became wider to ensure that the pressure loss was negligible compared to that in the other nanochannel parts, based on a theoretical model developed in a previous study.[34] Microchannels with width and depth dimensions of 500 μm and 6 μm interfaced with the nanochannel to permit sample injection were designed to provide a pressure loss that was sufficiently lower than the nanochannel. Therefore, when an external pressure was applied to the nanofluidic device during injection of the sample, the pressure applied to the nanochannel was approximately equal to the external pressure. The channel size effects were assessed by fabricating another nanofluidic device including a larger two-phase flow nanochannel with width and depth dimensions of 4000 nm and 2000 nm, based on a similar design concept.

The formation of parallel two-phase flow was verified in tests with pure water and dodecane as model aqueous and organic phases, respectively. These liquids were injected by the application of external pressure generated by two pressure controllers (PC20, Nagano Keiki Co., Ltd., Tokyo, Japan). Fluid flows

in the nanochannel were observed with an inverted microscope (IX71, Olympus Corp., Tokyo, Japan) combined with an oil immersion objective lens (100×, *NA* = 1.4) and an electron multiplying charge-coupled device (EMCCD) camera (C9100-13, Hamamatsu Photonics K. K., Hamamatsu, Japan).

3.3. Solvent extraction of a lipid

Utilizing the aqueous/organic two-phase flow in the nanochannel, the solvent extraction of a lipid based on the Bligh-Dyer method was demonstrated. The model sample was made from a 0.7 μmol/L solution of the lipid (Texas Red™ 1,2-dihexadecanoyl-*sn*-glycero-3-phosphoethanolamine triethylammonium salt; Texas-red-DHPE, Thermo Fisher Scientific Inc., MA, USA) and an 80 μmol/L solution of the amino acid (serine labeled with 4-fluoro-7-nitrobenzofurazan; NBD-F-Serine). Both the lipid and amino acid were dissolved in a two-to-one mixture of methanol and phosphate buffered saline (PBS), acting as the aqueous phase. Chloroform was used as the organic phase, acting as an extractant. The aqueous phase (including the sample) and the organic phase were injected into a two-phase flow nanochannel with width and depth dimensions of 1300 nm and 650 nm, that had been partially modified with ODS. The two-phase flow in the nanochannel was observed by bright-field inverted microscopy. The behavior of the lipid and amino acid in the nanochannel was separately monitored based on the fluorescence of the Texas-red (absorption: 589 nm, emission: 615 nm) and that of the NBD-F (absorption: 470 nm, emission: 530 nm) by changing the optical filters of the inverted microscope.

4. Results and Discussion

4.1. Partial hydrophobic surface modification of the nanochannel

Prior to device fabrication, the partial hydrophobic surface modification method utilizing FIB was evaluated. For this purpose, a nanochannel with width and depth dimensions of 4000 nm and 2200 nm for the proof-of-principle, and that of 150 nm and 60 nm were prepared. The FIB fabrication process illustrated in Fig. 1(b) was performed with an acceleration voltage of 40 kV, a beam current of 0.02 nA, a magnification of 40k×, a dwell time of 1.0 μs, and an aperture diameter of 30 μm. In this fabrication condition of FB2200, an etching depth of glass surface by FIB irradiation is expected to be suppressed to around 2 nm, which is similar to the thickness of ODS layer.[35] For the evaluation, the nanochannel surface was observed by field-emission scanning electron microscopy (SU8220, Hitachi High-Technologies Corp., Tokyo, Japan).

Figure 3 presents the result obtained following the partial hydrophobic surface modification of the 2200 nm nanochannel. As shown in Fig. 3(a), prior to the FIB ablation of the ODS region, a homogenous nanochannel surface was present. In the image acquired after the FIB ablation at an angle of 45° (Fig. 3(b)), part of the nanochannel surface (over a width of 1800 nm) is evidently brighter than the remaining 2200 nm wide region, which is equal to the nanochannel depth. Due to variation in the electron density at the surface, the SEM image of the ODS-modified surface appears darker compared to the glass surface. Hence these results suggest that the nanochannel functioned as a mask during the FIB ablation as proposed in this study, and the region over which the ODS was retained was in the shadow formed by the inclined nanochannel, while the ODS was removed from the area irradiated by the FIB. Therefore, we verified the

intended nanoscale partial hydrophobic surface modification of the nanochannel. As shown in Fig. 4, we also succeeded in the first-ever partial hydrophobic surface modification of a 60 nm nanochannel. According to the design, an ODS-modified surface with a width of 60 nm and a glass surface with a width of 90 nm width were patterned in the nanochannel. This was possible due to the very narrow FIB beam diameter of approximately 10 nm. As expected, the etching of glass surface by FIB was not confirmed obviously, and is considered to be negligibly small compared with the nanochannel depth.

4.2. Appearance of aqueous/organic parallel two-phase flow in the nanochannel

Based on this newly developed process, we succeeded in fabricating a nanofluidic device including a partially hydrophobic nanochannel based on the design illustrated in Fig. 2, and conducted experiments to verify the feasibility of this approach. Figure 5(a) provides a microscopic image of the aqueous/organic two-phase flow in the nanochannel having a width of 1500 nm and a depth of 890 nm and with partial hydrophobic modification. An image of flow in an unmodified glass nanochannel was also obtained for comparison purposes. In the case of the partially hydrophobic nanochannel, the water and dodecane meet at the confluence part, flow in parallel and then flow out along their respective downstream channels. This result confirms the appearance of aqueous/organic parallel two-phase flow in the nanochannel at a volume of 40 fL, together with the first-ever realization of phase confluence and phase separation as nano unit operations (NUOs). However, in the case of the unmodified nanochannel, the water and dodecane flow in an alternating manner to produce a plug flow phenomenon. These results indicate that the nanoscale partial hydrophobic modification is necessary to realize parallel two-phase flow.

Since the Laplace pressure works to maintain the liquid/liquid interface in the nanochannel with partial hydrophobic modification, parallel two-phase flow could be obtained even when the external pressures were set to be zero. Under this condition, we observed the shape of the water/dodecane interface in the depth-wise direction by changing the position of the focal plane of the objective lens. Figure 5(b) shows the results of these observations. Note that the focal plane depth was approximately 600 nm, as defined by the depth of field[36] calculated from the refractive index of immersion oil (1.515), the pixel size of the EMCCD camera (16 μm) and the properties of the objective lens. The top surface is seen to be almost fully wetted with the dodecane, while the bottom surface is wetted with both dodecane and water based on the hydrophobic/hydrophilic patterning of the surface. Thus, the top glass surface was relatively hydrophobic despite the absence of surface modification. As shown in Table 1, the contact angles of water and dodecane on the glass substrate were 0° and 21°, respectively, while those on the plasma-irradiated glass substrate were 15° and 0°, respectively. These results suggest that exposure to the oxygen and fluorine plasma for the purpose of low temperature bonding renders the glass surface hydrophobic and more wettable with dodecane compared to water. Therefore, within the nanochannel, the top glass and the ODS-modified surfaces make contact with the dodecane, while the other glass surfaces are in contact with water.

We further investigated the conditions under which parallel two-phase flow appears in the nanochannel with partial hydrophobic surface modification. These experiments were performed at external pressures ranging from 0 to 400 kPa, and the flow regime as a function of the external pressure

is plotted in Fig. 6(a). When the external pressures applied to the aqueous and organic phases were 0 and 400 kPa, respectively, the organic phase was the sole fluid flow and the channel was filled only with dodecane. Although the width of the aqueous phase in the parallel two-phase flow increased with increasing pressure applied to the aqueous phase as shown in captured images (Fig. 6(a)), parallel two-phase flow was observed at external pressure in excess of 100 kPa. Therefore, we verified stable control over the parallel two-phase flow as a result of the partial hydrophobic surface modification of the nanochannel, as was previously achieved in microchannels by our group.[24,25] This result also suggests that the parallel two-phase flow can be precisely controlled by changing external pressures. As shown in Fig. S1, by changing the external pressure at 50 kPa intervals, the proportion between the organic and aqueous phases could be gradually varied. For realizing precise control of the proportion between the two-phases, quantitative evaluation of the nanoscale flow configuration utilizing advanced observation methods such as super-resolution microscopy and confocal microscopy is required, and it is an issue in the future work.

The effect of the channel size was examined by assessing the flow regime in a nanochannel having a width of 4000 nm and a depth of 2000 nm together with partial hydrophobic surface modification, as shown in Fig. 6(b). Similar to the results obtained in the 890 nm nanochannel, we succeeded in forming aqueous/organic parallel two-phase flow in the larger nanochannel at a volume of 240 fL. With increasing external pressure applied to the aqueous phase, the flow regime changed from an organic phase flow, to a parallel two-phase flow, and finally an aqueous phase flow, as shown in captured images (Fig. 6(b)). It should also be noted that plug flow was not observed. Compared to the results obtained with the smaller

nanochannel (Fig. 6(a)), the fluid flows were unstable and range of pressure over which parallel two-phase flow appeared was narrower. In particular, the water/dodecane interface was distorted to a greater extent with changes in the fluid pressure along the channel due to pressure loss. This tendency occurred in the 2000 nm nanochannel was a result of the weakened effect of the surface tension that worked to maintain the liquid/liquid interface, because the Laplace pressure was lower than that in the 890 nm nanochannel by a factor of 2.2 because of the larger channel size. Although unique wetting phenomena of water confined in nm spaces different from the bulk have been reported[37] and it can affect the flow regime when the channel size becomes 1-10 nm, the results obtained in this study suggest that the partial hydrophobic surface modification generated a more stable aqueous/organic parallel two-phase flow in smaller nanochannels.

To verify contribution of the Laplace pressure to keep the parallel two-phase flow, we estimated the Laplace pressure in the nanochannels from the advance and receding contact angles of water in dodecane on surfaces, measured by the contact angle meter as listed in Table 2. Noted that our previous study revealed that wetting property of water in 100 nm glass nanochannels is similar to that in the bulk.[38] From the dynamic contact angles and the surface tension at water/dodecane interface of 52.8 mN/m, a range of the Laplace pressure was estimated to be -76 kPa $\leq P_{LP} \leq$ 66 kPa in the 890 nm nanochannel, and -34 kPa $\leq P_{LP} \leq$ 30 kPa in the 2000 nm nanochannel, based on the Young-Laplace equation modified for nonuniform surfaces.[39] Considering a balance between the Laplace pressure, P_{LP}, and the fluid pressure, P_f, in the parallel two-phase flow as shown in Fig. 1(a), a range of the fluid pressure allowed for the

parallel two-phase flow is -66 kPa $\leq P_f \leq 76$ kPa in the 890 nm nanochannel, and -30 kPa $\leq P_{LP} \leq 34$ kPa in the 2000 nm nanochannel, indicated as yellow area in Fig. 6. Here, the external pressures to the aqueous and organic phases were converted to those to the aqueous, P_{aq}, and organic phases, P_{org}, at the phase confluence point to approximately calculate the fluid pressure by $P_f = P_{aq} - P_{org}$, considering the pressure loss with the lengths of the inlet nanochannel, the two-phase flow nanochannel, and the interface nanochannel connected to the taper-shaped nanochannel. As shown in Fig. 6, the pressure ranges of the parallel two-phase flow obtained by the experiments roughly correspond to those predicted from the dynamic contact angles. This result further supports the formation of the parallel two-phase flow in nanochannels by the Laplace pressures controlled by the hydrophobic/hydrophilic surface patterning.

4.3. Solvent extraction of a lipid

The fL scale solvent extraction of a lipid via the Bligh-Dyer method was demonstrated utilizing the aqueous/organic parallel two-phase flow in the nanochannel. Figure 7(a) shows a bright-field image of two-phase flow by the PBS/methanol mixture and chloroform in the nanochannel. This image confirms that parallel two-phase flow at a volume of 25 fL was successfully generated as a result of the partial hydrophobic surface modification. This flow was possible due to the difference in solvent wettability on the ODS-modified surface (such that the contact angles of the methanol/PBS and chloroform on this surface were 55° and 18°, while those on the glass surface were 10° and 9°, respectively, as shown in Table 1). However, the image of an interface between the PBS/methanol mixture (n = 1.34) and chloroform (n = 1.44) in the parallel two-phase flow is not clear compared with that between water (n =

1.33) and dodecane (n = 1.42) shown in Figure 5(a), where n is the refractive index given by a literature,[40] despite almost similar difference in the refractive index between the aqueous and organic phases in these two cases. This is probably because methanol included in the aqueous phase, which is miscible with chloroform, mixed into the organic phase, as well known in the Bligh-Dyer method.

The behavior of solute molecules in this parallel two-phase flow is shown in Fig. 7(b). As expected based on the principle of the Bligh-Dyer method, the lipid was extracted into the organic phase while the amino acid remained in the aqueous phase. Since the fluorescence of the Texas-red was significantly decreased in the organic phase owing to a reduction in the quantum yield due to a dye-solvent interaction,[41] quantification of the extraction efficiency was difficult. However, the observed qualitative difference in fluorescence intensity between the organic and aqueous phase outlets suggests highly-efficient separation of the lipid and amino acid. These results confirm the first-ever successful integration of solvent extraction into a nanochannel as a result of three NUOs: phase confluence, extraction, and phase separation.

Because the fluorescent zone associated with the Texas-red moved from the aqueous phase to the organic phase at a position approximately 10 μm-downstream from the phase confluence point (Fig. 7(b)), the minimum sample volume required was around 4 fL and the time necessary for the extraction was approximately 1 ms, based on the estimated velocity of the aqueous phase with the viscosity of methanol/water solution.[42] Therefore, using the effects of a very small scale and the dominance of diffusion effects in a nanochannel, solvent extraction was accomplished in a volume 250 times smaller

than that of a single cell (1 pL), with a processing time 10,000 times faster than that achieved by parallel multiphase microfluidics.[9,10] As the Bligh-Dyer method is a broadly used pretreatment processing in cell analysis in the field of lipidomics,[43,44] this fL-scale lipid extraction is expected to contribute to the development of single cell lipidomics utilizing nanofluidics. In addition, this stable parallel two-phase flow on the fL volume scale should enable the integration of various chemical processing to achieve chemical applications with ultra-small amounts of molecules (even countable quantities) as a result of connecting various NUOs. Accordingly, this study represents a technical breakthrough to realize parallel multiphase nanofluidics for chemical analyses and syntheses of ultra-small amounts of molecules.

5. Conclusions

This work developed a nanoscale partial hydrophobic modification method to realize aqueous/organic parallel two-phase flow in nanochannels, and demonstrated fL-scale solvent extraction. Utilizing FIB and the nanochannel itself as a mask by inclining the substrate, partial hydrophobic surface modification was achieved even in a 60 nm nanochannel. This technique enables nanoscale patterning of various molecules on surfaces of not only nanochannels but also various three-dimensional nanostructures. Utilizing this newly developed method, the formation of water/dodecane parallel two-phase flow in a nanochannel was verified even when the external pressures used to drive the fluids were set to zero. The results suggest that hydrophobic surface patterning, which allows the liquid/liquid interface to be maintained by the Laplace pressure, is necessary in order to obtain parallel two-phase flow in a

nanochannel. Finally, by integrating the NUOs of phase confluence, extraction and phase separation, solvent extraction of a lipid according to the Bligh-Dyer method was demonstrated. Specifically, ultra-small (4 fL) and high-speed (1 ms) separation of a lipid and an amino acid was demonstrated, utilizing the parallel two-phase flow of methanol/PBS and chloroform. Since the Bligh-Dyer method is a broadly used pretreatment processing in lipidomics, this work suggests the viability of single cell analysis utilizing parallel multiphase nanofluidics. This study is expected to make a significant contribution to the field of nanofluidics by allowing the integration of various chemical processing for ultra-small quantities of molecules. The techniques demonstrated herein could result in novel applications, such as research tools for the investigation of nanoscale interfacial phenomena and analyses of single cells or even molecules.

Conflicts of Interest

There are no conflicts of interest to declare.

Acknowledgement

The authors gratefully acknowledge financial support from the Core Research for Evolutional Science and Technology (CREST) of the Japan Science and Technology Agency (JST): JPMJCR14G1. Some of the fabrication facilities were provided from the Academic Consortium for Nano and Micro Fabrication by four Universities (Keio University, Waseda University, Tokyo Institute of Technology, and The University of Tokyo, Japan).

References

1 A. Günther and K. F. Jensen, *Lab Chip*, 2006, **6**, 1487-1503.

2 A. Aota, K. Mawatari and T. Kitamori, *Lab Chip*, 2009, **9**, 2470-2476.

3 K. Mawatari, Y. Kazoe, A. Aota, T. Tsukahara, K. Sato and T. Kitamori, *J. Flow Chem.*, 2011, **1**, 3-12.

4 S.A. Khan, A. Günther, M.A. Schmidt and K. F. Jensen, *Langmuir*, 2004, **20**, 8604-8611.

5 A. Larrea, V. Sebastian, A. Ibarra, M. Arruebo and J. Santamaria, *Chem. Mater.*, 2015, **27**, 4254-4260.

6 T.S. Kaminski and P. Garstecki, *Chem. Soc. Rev.*, 2017, **46**, 6210-6226.

7 M.T. Guo, A. Rotem, J.A. Heyman, D.A. Weitz, *Lab Chip*, 2012, **12**, 2146-2155.

8 M. Tokeshi, T. Minagawa, K. Uchiyama, A. Hibara, K. Sato, H. Hisamoto and T. Kitamori, *Anal. Chem.*, 2002, **74**, 1565-1571.

9 M. Tokeshi, T. Minagawa and T. Kitamori, *J. Chromatogr. A*, 2000, **894**, 19-23.

10 M. Tokeshi, T. Minagawa and T. Kitamori, *Anal. Chem.*, 2000, **72**, 1711-1714.

11 U. Novak, A. Pohar, I. Plazl, P. Žnidaršič-Plazl, *Separation and Purification Technology*, 2012, **97**, 172-178.

12 R.J. Meagher, Y.K. Light and A.K. Singh, *Lab Chip*, 2008, **8**, 527-532.

13 V. Reddy and J.D. Zahn, *J. Colloid Interface Sci.*, 2005, **286**, 158-165.

14 H. Hisamoto, Y. Shimizu, K. Uchiyama, M. Tokeshi, Y. Kikutani, A. Hibara and T. Kitamori, *Anal. Chem.*, 2003, **75**, 350-354.

15 A. Hibara, T. Saito, H.-B. Kim, M. Tokeshi, T. Ooi, M. Nakao and T. Kitamori, *Anal. Chem.*, 2002, **74**, 6170-6176.

16 K. Mawatari, Y. Kazoe, H. Shimizu, Y. Pihosh and T. Kitamori, *Anal. Chem.*, 2014, **86**, 4068-4077.

17 K. Shirai, K. Mawatari, R. Ohta, H. Shimizu and T. Kitamori, *Analyst*, 2018, **143**, 943-948.

18 B. R. Cipriany, P. J. Murphy, J. A. Hagarman, A. Cerf, D. Latulippe, S. L. Levy, J. J. Benítez, C. P. Tan, J. Topolancik, P. D. Soloway and H. G. Craighead, *PNAS*, 2012, **109**, 8477-8482.

19 R. Ishibashi, K. Mawatari and T. Kitamori, *Small*, 2012, **8**, 1237-1242.

20 Y. Pihosh, Y. Kazoe, K. Mawatari, H. Seo, O. Tabata, T. Tsuchiya, K. Kitamura, M. Tosa, I. Turkevych and T. Kitamori, *Adv. Mater. Technol.*, 2019, 1900252.

21 F. Malloggi, N. Pannacci, R. Attia, F. Monti, P. Mary, H. Willaime and P. Tabeling, *Langmuir*, 2010, **26**, 2369-2373.

22 L. Shui, A. van den Berg and J.C.T. Eijkel, *Microfluid Nanofluid*, 2011, **11**, 87-92.

23 R. Arayanarakool, L. Shui, S. W. M. Kengen, A. van den Berg and J. C. T. Eijkel, *Lab Chip*, 2013, **13**, 1955-1962.

24 A. Hibara, S. Iwayama, S. Matsuoka, M. Ueno, Y. Kikutani, M. Tokeshi and T. Kitamori, *Anal. Chem.*, 2005, **77**, 943-947.

25 A. Aota, M. Nonaka, A. Hibara and T. Kitamori, *Angew. Chem. Int. Ed.*, 2007, **46**, 878-880.

26 B. Zhao, J.S. Moore and D.J. Beebe, *Science*, 2001, **291**, 1023-1026.

27 K. Shirai, K. Mawatari and T. Kitamori, *Small*, 2014, **10**, 1514-1522.

28 K. Sugioka, J. Xu, D. Wu, Y. Hanada, Z. Wang, Y. Cheng and K. Midorikawa, *Lab Chip*, 2014, **14**, 3447-3458.

29 B. Xu, Y. Shi, Z. Lao, J. Ni, G. Li, Y. Hu, J. Li, J. Chu, D. Wu and K. Sugioka, *Lab Chip*, 2018, **18**, 442-450.

30 D.S. Ginger, H. Zhang and C.A. Mirkin, *Angew. Chem. Int. Ed.*, 2004, **43**, 30-45.

31 E.G. Bligh and W.J. Dyer, *Can. J. Biochem. Physiol.*, 1959, **37**, 911-917.

32 T. Tsukahara, K. Mawatari, A. Hibara and T. Kitamori, *Anal. Bioanal. Chem.*, 2008, **391**, 2745-2752.

33 Y. Xu, C. Wang, L. Li, N. Matsumoto, K. Jang, Y. Dong, K. Mawatari, T. Suga and T. Kitamori, *Lab Chip*, 2013, **13**, 1048-1052.

34 K.-S. Yang, I.-Y. Chen, B.-Y. Shew and C.-C. Wang, *J. Micromech. Microeng.*, 2004, **14**, 26-31.

35 H. Sugimura, A. Hozumi, T. Kameyama and O. Takai, *Surf. Interface Anal.*, 2002, **34**, 550-554.

36 S. Inoué and K.R. Spring, *Video Microscopy: The Fundamentals*, 2nd Ed, Springer, 1997.

37 Z. YaHong, G. Wei and J. Lei, *Sci. China-Phys. Mech. Astron.*, 2014, **57**, 836-843.

38 L. Li, Y. Kazoe, K. Mawatari, Y. Sugii and T. Kitamori, *J. Phys. Chem. Lett.*, 2012, **3**, 2447-2452.

39 W. Huang, Q. Liu and Y. Li, *Chem. Eng. Technol.*, 2006, **29**, 716-723.

40 M.D. Lechner, Ed., *Optical Constants – Refractive Indices of Pure Indices of Pure Liquids and Binary Liquid Mixtures (Supplement to III/38)*, in *Landolt-Börnstein – Group III Condensed Matter*,

Springer Nature Switzerland AG, 2008.

41 M. Beija, C.A.M. Afonso and J.M.G. Martinho, *Chem. Soc. Rev.*, 2009, **38**, 2410-2433.

42 S.Z. Mikhail and W.R. Kimel, *J. Chem. Eng. Data*, 1961, **6**, 533-537.

43 T. Cajka and O. Fiehn, *Anal. Chem.*, 2016, **88**, 524-545.

44 R. Taguchi, T. Houjou, H. Nakanishi, T. Yamazaki, M. Ishida, M. Imagawa and T. Shimizu, *J. Chromatogr. B*, 2005, **823**, 26-36.

Table of Contents Entry

Aqueous/organic parallel two-phase flow in a nanochannel was realized by developing a nanoscale partial hydrophobic surface modification method, and applied to solvent extraction of lipid at femtoliter sample volume and millisecond processing time.

Tables

Table 1. Static contact angle of solvents in air on surfaces

	Water	Dodecane	PBS/methanol	Chloroform
Glass surface	0°	21°	10°	9°
Plasma-irradiated glass surface	15°	0°	47°	18°
ODS-modified surface	110°	0°	55°	18°

Table 2. Dynamic contact angle of water in dodecane on surfaces

	Advance contact angle	Receding contact angle
Glass surface	68°	22°
Plasma-irradiated glass surface	116°	79°
ODS-modified surface	148°	28°

Figure Captions

Figure 1. Schematics of (a) the method of generating aqueous/organic parallel two-phase flow in a nanochannel with partial hydrophobic surface modification and (b) a technique for the partial hydrophobic surface modification of the nanochannel utilizing FIB.

Figure 2. Schematic of the experimental setup for the nanofluidic device including a nanochannel having a width of 1590 nm and a depth of 890 nm with partial hydrophobic surface modification by ODS.

Figure 3. Schematics and FE-SEM images of (a) a nanochannel (width: 4000 nm, depth: 2200 nm) modified by ODS and (b) the same channel after partial hydrophobic surface modification by FIB.

Figure 4. A schematic and FE-SEM images of a nanochannel (width: 150 nm, depth: 60 nm) following partial hydrophobic surface modification by FIB.

Figure 5. Observation of water/dodecane two-phase flow in a nanochannel. (a) Parallel two-phase flow in a nanochannel with partial hydrophobic surface modification with external pressures of 250 and 350 kPa applied to the organic and aqueous phases, and a plug flow in an unmodified glass nanochannel at external pressures of 250 and 250 kPa. (b) The water/dodecane interface in a nanochannel with partial hydrophobic surface modification as observed at different depths with the external pressures to the organic and aqueous phases set to zero.

Figure 6. Fluid flow regimes as functions of the external pressures applied to the aqueous and organic phases in nanochannel with (a) a width of 1500 nm and a depth of 890 nm and (b) a width of 4000 nm and a depth of 2000 nm, following partial hydrophobic surface modification. Yellow area indicates a range of external pressures allowed for the parallel two-phase flow, predicted from the Laplace pressure calculated using the dynamic contact angles as listed in Table 2. In the case of the larger nanochannel (width: 4000 nm, depth: 2000 nm), applying an external pressure of zero to the aqueous or organic phase or to both gave an irreproducible flow regime due to unstable fluid flow. Hence, the flow regimes under these conditions are not plotted.

Figure 7. Results for solvent extraction of a lipid in a nanochannel. (a) Aqueous/organic parallel two-phase flow in the nanochannel as observed by bright-field imaging. (b) Behavior of a lipid and an amino acid in the parallel two-phase flow, separately observed by changing the fluorescence wavelength monitored by the EMCCD camera. The lipid (Texas-red-DHPE) and amino acid (NBD-F-serine) were tracked based on red and green fluorescence, respectively, and the fluorescence intensities at the phase confluence point and the channel outlets are indicated in arbitrary units.

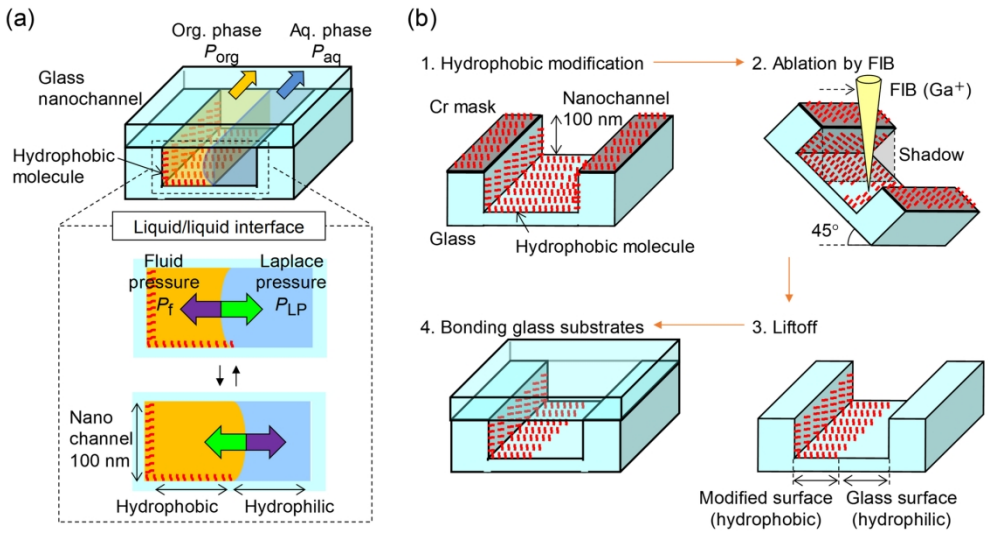

Figure 1

173x92mm (300 x 300 DPI)

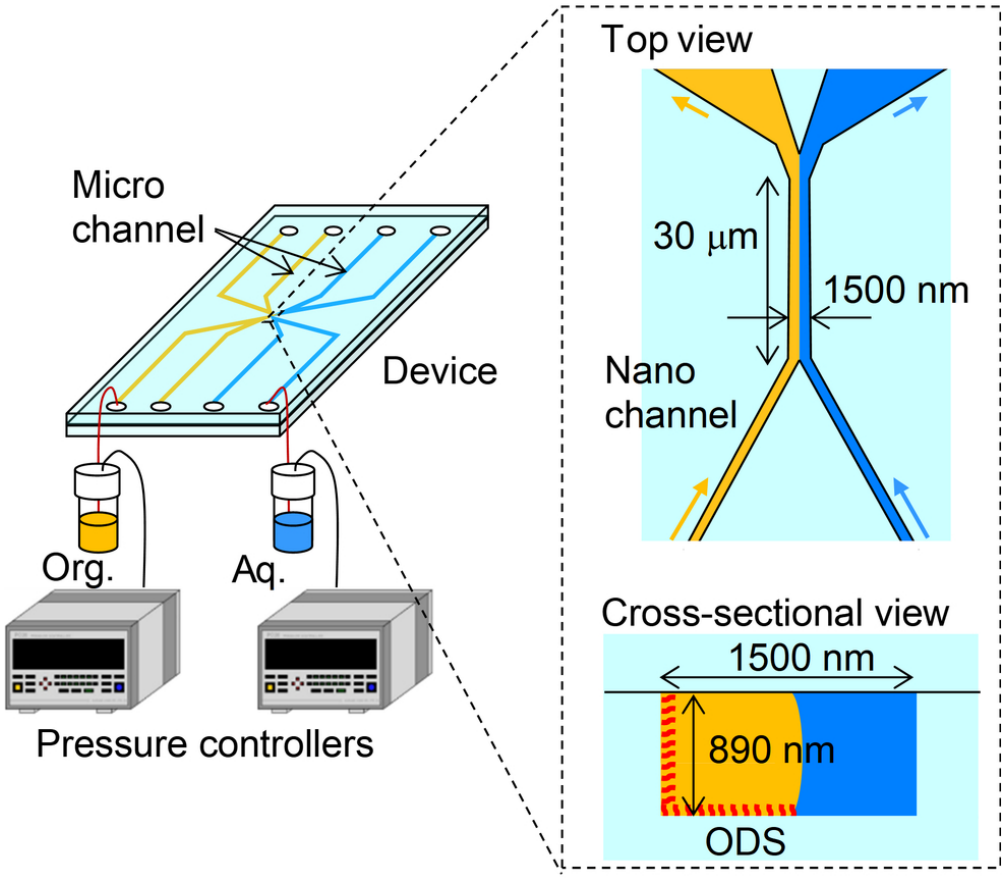

Figure 2

83x73mm (300 x 300 DPI)

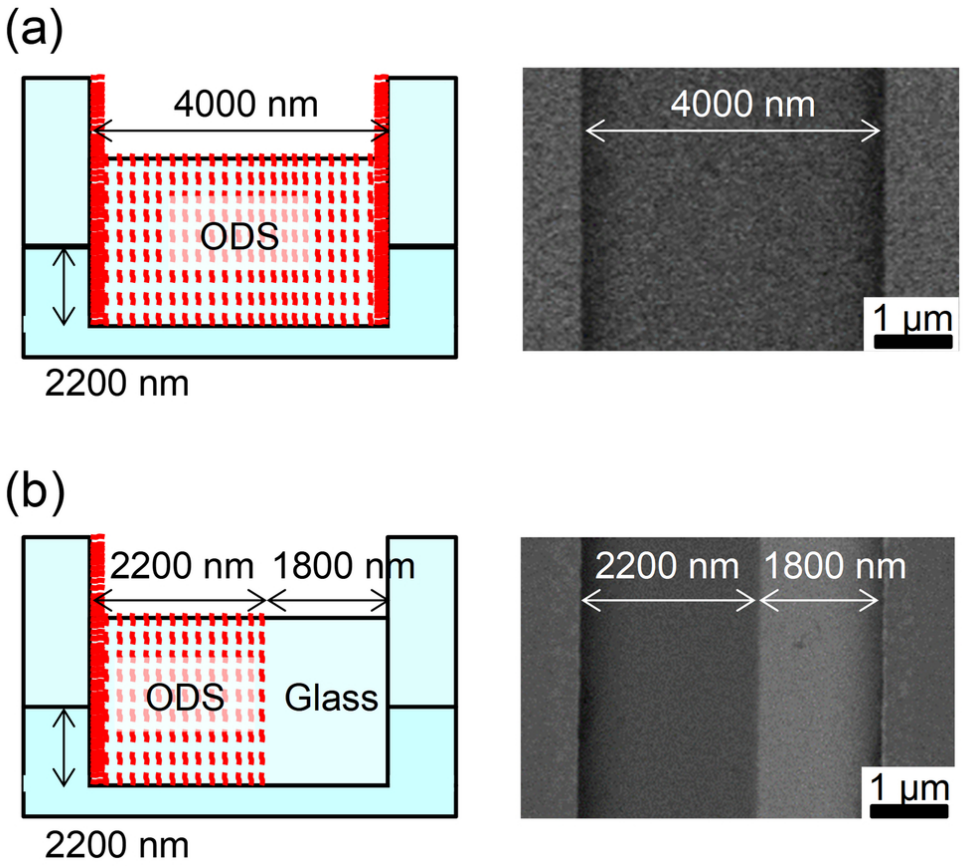

Figure 3

85x75mm (300 x 300 DPI)

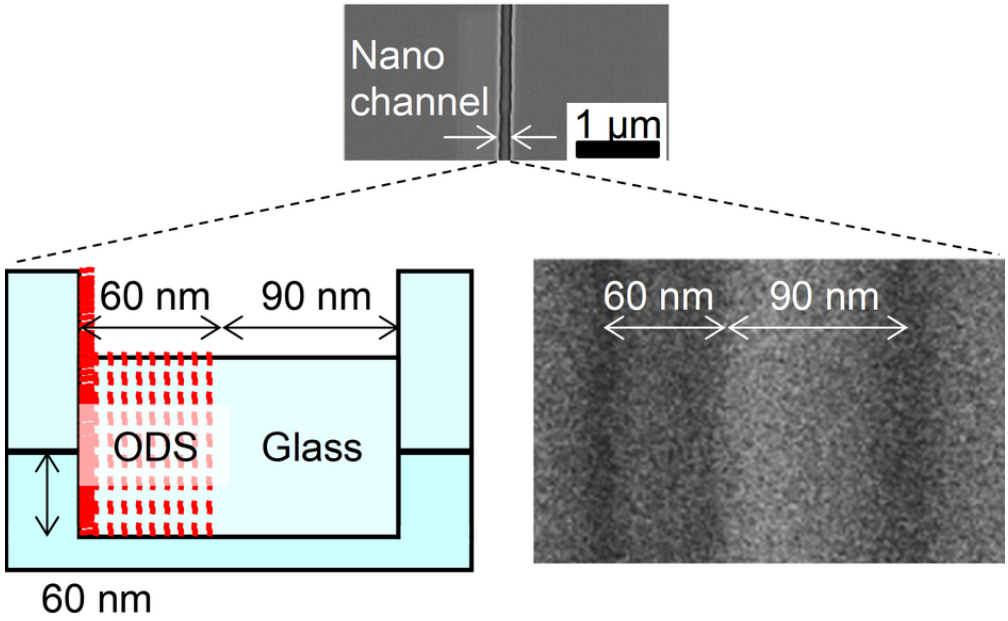

Figure 4

79x50mm (300 x 300 DPI)

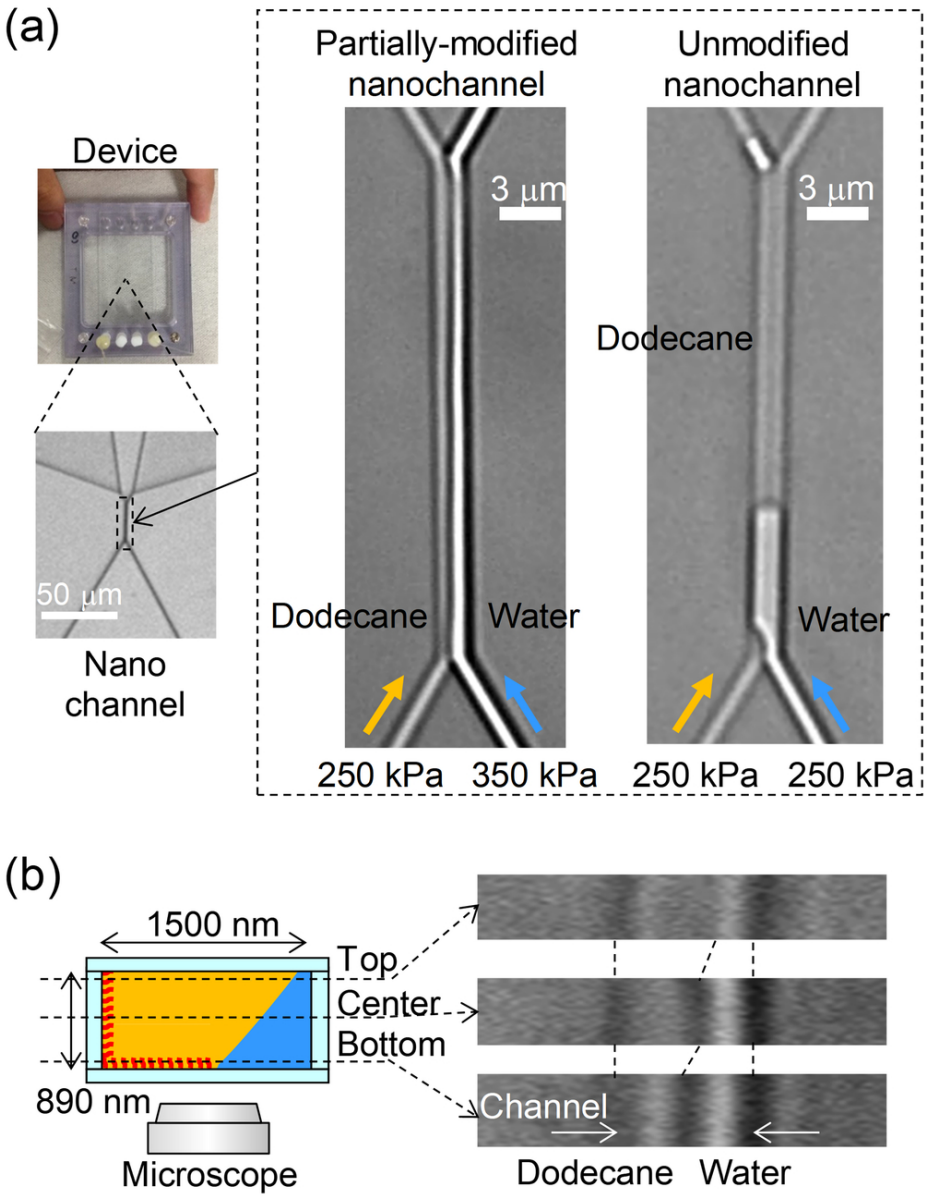

Figure 5

85x109mm (300 x 300 DPI)

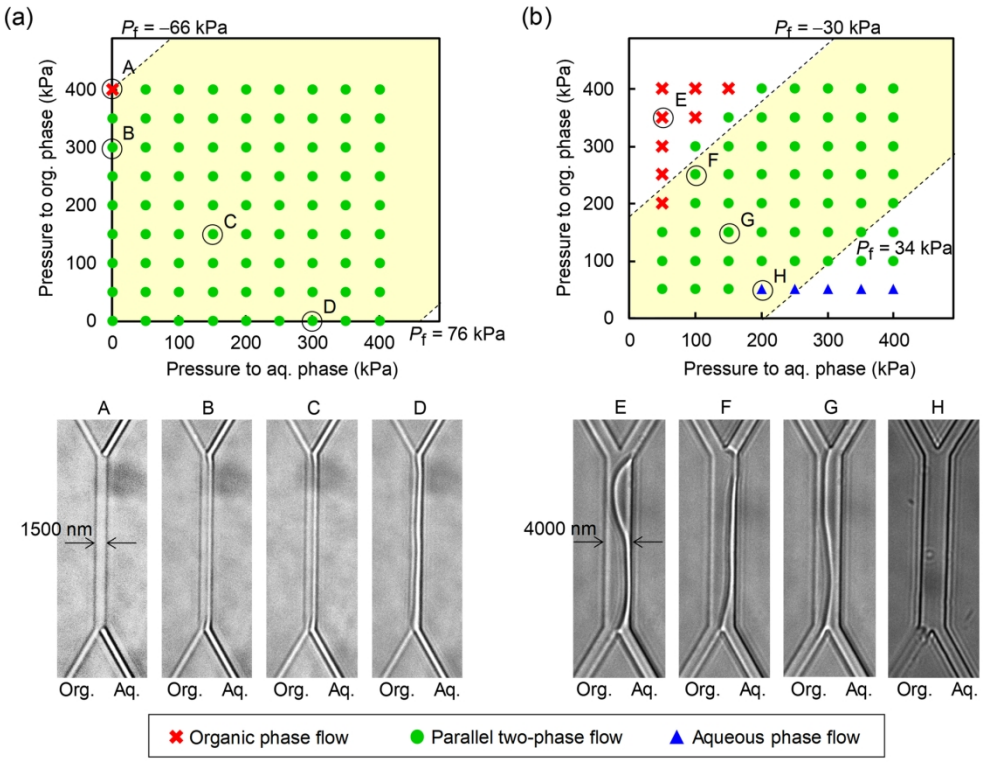

Figure 6

170x130mm (300 x 300 DPI)

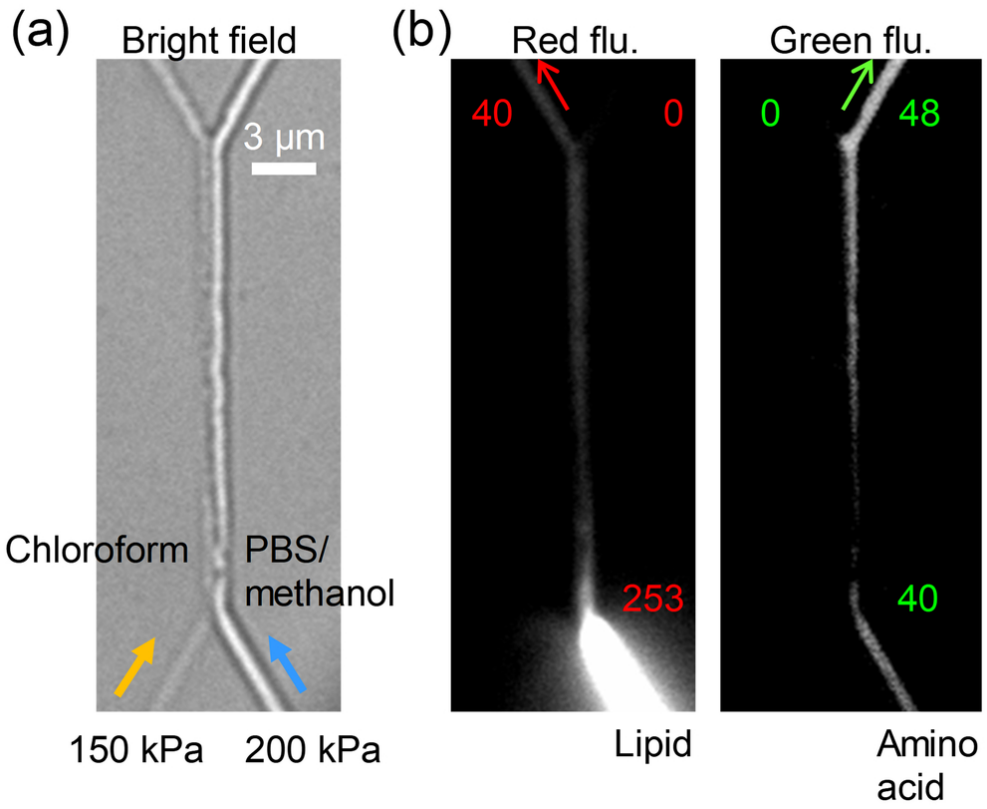

Figure 7

85x70mm (300 x 300 DPI)

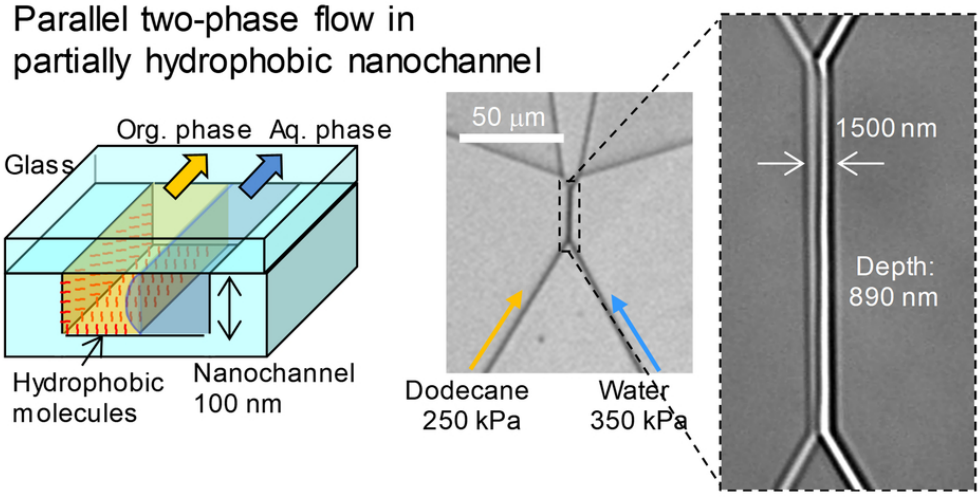

79x39mm (300 x 300 DPI)